Atmospheric Environment 190 (2018) 284–293

Contents lists available at ScienceDirect

Atmospheric Environment

journal homepage: www.elsevier.com/locate/atmosenv

Intake fraction estimates for on-road fine particulate matter ($PM_{2.5}$) emissions: Exploring spatial variation of emissions and population distribution in Lisbon, Portugal

Joana Bastos[a,b,*], Chad Milando[b], Fausto Freire[a], Stuart Batterman[b]

[a] ADAI-LAETA, Department of Mechanical Engineering, University of Coimbra, Portugal
[b] Department of Environmental Health Sciences, University of Michigan, USA

ARTICLE INFO

Keywords:
Air pollution
Fine particulate matter ($PM_{2.5}$)
Intake fraction
Population exposure
Road emissions

ABSTRACT

The intake fraction (iF) expresses population exposure resulting from pollutant emissions. City-wide iFs estimated using simple one-compartment models, which have been used in a number of previous studies, have significant uncertainties and do not capture the intra-urban variation in exposure that is important for estimating health effects associated with traffic-related air pollutants. We present a novel and efficient approach for developing spatially-resolved iF estimates using dispersion modeling for near-road exposures that accounts for the spatial and temporal variation in meteorology, emissions and the population living and working near major roads. Using the new approach, iF estimates are developed for emissions of traffic-related fine particulate matter ($PM_{2.5}$) in Lisbon, Portugal, and compared to estimates from a one-compartment model. Both methods use local meteorological and population data and represent exposures for a total of 2.8 million people. The new method produces an overall iF value of 16.4 ppm for the Lisbon metropolitan area, over twice that of the one-compartment model (8.1 ppm). Most of the exposure (12.0 ppm) occurs for the subset of the population (1.0 million people) living or working within 500 m of highways and major arterials. The iF for the remainder of the population (1.8 million people) is only 4.3 ppm. The spatially-resolved iF estimate accounts for high concentration areas, which can be densely populated, and accounts for much or most of the exposure from traffic-related emissions. The new method is computationally efficient and can improve estimates of exposure and health impacts occurring in urban areas, leading to more effective urban and transportation planning decisions to mitigate impacts.

1. Introduction

Exposure to airborne particulate matter (PM) has been associated with severe health impacts, including reduced life expectancy, respiratory and cardiovascular morbidity (e.g., aggravation of asthma, respiratory problems and increased hospital admissions), and cardiopulmonary and lung cancer mortality (World Health Organization, 2003, 2013; 2016; Lim et al., 2012). In Europe, over 80% of urban dwellers are currently exposed to fine particulate matter ($PM_{2.5}$) concentrations above the World Health Organization (WHO) guideline of 10 $\mu g/m^3$ (Shneider et al., 2014; EEA, 2017), and $PM_{2.5}$ has been estimated to cause over 300 000 premature deaths annually (Watkiss et al., 2005; EEA, 2017). Road transportation is one of the main contributions to $PM_{2.5}$ in urban areas, and locations near major roads have been associated with high exposures (Karagulian et al., 2015; Tainio et al., 2014).

The intake fraction (iF) expresses the fraction of a pollutant emitted from one or more sources that is inhaled by a defined population (Bennett et al., 2002; Marshall and Nazaroff, 2006; Stevens et al., 2007). City-wide iFs have been estimated using one-compartment models for cities worldwide that exceed 100 000 inhabitants (Stevens et al., 2007; Apte et al., 2012). These iF estimates can have significant uncertainty (Marshall et al., 2003; Stevens et al., 2007; Apte et al., 2012), and they do not account for the spatial (or intra-urban) variation in concentrations and exposures that may be important for predicting health impacts (Marshall et al., 2005; Greco et al., 2007a; Tainio et al., 2014; Lobscheid et al., 2012; Requia, Dalumpines et al., 2017). Such variation is especially important for traffic-related air pollutants (Greco et al., 2007a; Tainio et al., 2014). While several studies have explored the intra-urban spatial variation from specific emission sources (e.g., on-road traffic, power generation facilities, domestic combustion; Heath et al., 2006; Greco et al., 2007a; Greco et al., 2007b; Loh et al.,

* Corresponding author. ADAI-LAETA, Department of Mechanical Engineering, University of Coimbra, Rua Luís Reis Santos, 3030-788 Coimbra, Portugal, .
E-mail address: joana.bastos@dem.uc.pt (J. Bastos).

https://doi.org/10.1016/j.atmosenv.2018.07.037
Received 12 February 2018; Received in revised form 3 July 2018; Accepted 21 July 2018
Available online 23 July 2018
1352-2310/

2009; Lobscheid et al., 2012; Tainio et al., 2014; Lamancusa et al., 2017), these studies have been limited by coarse spatial resolution and, in cases, they lacked spatially-disaggregated emission data.

This paper presents a novel approach for determining iFs that account for the intra-urban variation of exposures. Spatially-resolved iF estimates are derived by combining dispersion modeling and geographic information systems (GIS) in an efficient and scalable manner that accounts for the spatial and temporal variation in meteorological conditions, pollutant emissions and population distributions. We present an application for primary $PM_{2.5}$ road emissions for the Lisbon, Portugal, metropolitan area. Results are compared with a one-compartment model iF estimate and the literature.

2. Background

2.1. Intake fractions for traffic-related air pollution

Several methods have been used to estimate iFs for traffic-related air pollutants, including one-compartment box models and air quality dispersion models. One-compartment or "box" models provide a simple approach that uses just a few parameters to account for key factors (Marshall et al., 2003; Stevens et al., 2007). Air quality dispersion models, discussed later, provide a more sophisticated approach that can predict spatially- and temporally-resolved concentration estimates; however, these models are complex and require extensive input data, and computational requirements can be large (Stevens et al., 2007).

2.1.1. City-scale intake fractions using one-compartment models

One-compartment models assume that pollutant emissions are dispersed into a single fully-mixed compartment, representing a highly simplified approach with few data requirements. These models provide some insight on the influence of several variables affecting population exposure to non-reactive air pollutants, specifically, the model domain or area, population, dilution rates (i.e., the product of wind speed and mixing height), and breathing rates (Stevens et al., 2007). Table 1 summarizes parameters and results in five studies using city-scale applications of one-compartment models to estimate iFs. In an early study exploring sensitivity to a wide set of parameters in archetype environments, the urban area ranged from 100 to 10 000 km^2 and population from 0.6 to 60 million people, giving dilution rates from 300 to 3000 m^2/s and iFs from 4.4 to 440 ppm (Lai et al., 2000). A study focusing on working-age population in Helsinki estimated a iF of only 7 ppm (Loh et al., 2009), largely due to the low population density (663 km^{-2}) that resulted from the age group selected (22–55 years old, 46% of the metropolitan area population). Other studies have used population densities from 1712 to 8330 km^{-2}, dilution rates from 270 to 610 m^2/s, and breathing rates from 13 to 20 m^3/d (Stevens et al., 2007; Humbert et al., 2011; Apte et al., 2012). City-specific population and meteorology for Mexico City gave a very high iF of 120 ppm (Stevens et al., 2007). In a study covering 3646 cities worldwide, the population-weighted iF averaged 39 ppm (range of 0.6–260 ppm, and small, medium and large cities (populations of 0.1–0.6, 0.6–3.0, and over 3 million inhabitants) had population-weighted average iFs of 15, 35 and 65 ppm, respectively (Apte et al., 2012). Humbert et al. (2011) separated emission sources by height (ground-level, low- and high-stack), based on literature-derived data, and estimated an average iF of 26 ppm for an archetypal urban area, about half of that for ground level sources (44 ppm). To better compare results in the literature, we calculated iFs on a per person basis, referred to as $iF_{personal}$, for the five studies (Table 1). This metric shows a tighter range (9–22 parts per trillion, ppt), excluding the parametric sensitivity analysis performed by Lai et al. (2000).

City-wide iF estimates using one-compartment models have limitations. Estimates strongly depend on the spatial domain selected, e.g., increasing the domain size can dilute emissions into a larger volume and thus lower the iF. Conversely, restricting the domain to high density land uses can inflate the iF (Lamancusa et al., 2017). Other limitations include a lack of spatial resolution (Stevens et al., 2007; Apte et al., 2012) and the steady-state assumption (e.g., constant emissions across the day), which is often applied.

2.1.2. Spatially-resolved intake fraction estimates

Air quality dispersion models allow spatially- and temporally-resolved predictions of concentrations, which can be used to estimate iFs that vary by region, season and emission source. Table 2 summarizes six prior studies that used dispersion models to consider spatial variability in iF estimates. In the USA, iFs for mobile source primary and secondary $PM_{2.5}$ emissions were estimated for 3080 counties using the Climatological Regional Dispersion Model (CRDM) (Greco et al., 2007b). iF estimates ranged from 0.12 to 25 ppm (mean of 1.6 ppm); and half of the total intake occurred within a median distance of 150 km for primary $PM_{2.5}$, and within 390–740 km for secondary $PM_{2.5}$. The authors concluded that long range dispersion models with coarse spatial resolution can be used to evaluate exposure to traffic-related primary $PM_{2.5}$ emissions in rural or remote areas and for secondary $PM_{2.5}$, but higher resolution is needed for traffic-related primary $PM_{2.5}$ in dense urban areas since much of the total intake occurs near the source. In Boston, Massachusetts, intra-urban variability (due to population distribution) in iFs for primary $PM_{2.5}$ road emissions was explored using the CAL3QHCR short-range dispersion model for populations up to 5 km from the road (Greco et al., 2007a). This analysis assumed the same emission rates across the 23 398 road segments and obtained a mean iF of 12 ppm (hourly values from 0.8 to 53 ppm). Regional and seasonal variations in iFs for primary and secondary PM emissions across the USA were calculated using source apportionments and the Comprehensive Air quality Model with Extensions (CAMx) regional air quality model (Lamancusa et al., 2017). The analysis considered spatially differentiated emissions and population densities to estimate

Table 1
Summary of iF estimates and associated parameters for urban areas using one-compartment steady-state models from five studies. $IF_{personal}$ (last column) facilitates comparison between studies.

	Domain	Area (km^2)	Width (km)	Population (10^3)	Population density (km^{-2})	Breathing rate (m^3/d)	Dilution rate (m^2/s)	iF (ppm)	$iF_{personal}$ (ppt)
Apte et al. (2012)	3646 cities worldwide	610[a]	24.7[a]	4.2[a]	6885[a]	14.5[a]	540[a]	39[a]	9.2[a]
Humbert et al. (2011)	Urban area archetype	240	15.5	2.0	8300	13.0	610	44/26[b]	22.1/13.1[b]
Loh et al. (2009)	Helsinki metro area	745	27.3	0.5[c]	663	19.9	600	7	14.1
Stevens et al. (2007)	Mexico city metro area	5022	71	8.6	1712	20.0	270	120	13.9
Lai et al. (2000)	Urban area archetype	100	10	0.6	6000	18.7	300–3000	4.4–44	7.3–73.3
Lai et al. (2000)	Urban area archetype	900	30	5.4	6000	18.7	300–3000	13–130	2.4–24.1
Lai et al. (2000)	Urban area archetype	10000	100	60.0	6000	18.7	300–3000	44–440	0.7–7.3

[a] Population weighted mean values.
[b] Ground level iF/emission-height-weighted iF.
[c] Working-age population.

Table 2
Overview of previous iF estimates using spatially-resolved approaches: summary of main model characteristics, methods and results. CRDM – Climatological Regional Disperion Model; CAMx – Comprehensive Air quality Model with Extensions; EXPAND – Exposure to air pollution, especially to nitrogen dioxide and particulate matter; CAR-FMI - Contaminants in the Air from a Road - Finish Meteorological Institute; iD75 - distance required for the cumulative iF to each 75% of its total.

Study	Domain	Pollutants	Sources	Methods	iFs/main results
Greco et al., 2007a	Boston, USA	primary $PM_{2.5}$	Traffic	CAL3QHCR line-source short-range dispersion model	0.8–53 ppm (mean: 12)
Greco et al., 2007b	USA (3080 counties)	primary and secondary $PM_{2.5}$	On-road mobile	CRDM dispersion model	primary $PM_{2.5}$: 0.12–25 ppm (mean: 1.6) Secondary $PM_{2.5}$: 0.001–10 ppm
Loh et al., 2009	Helsinki, Finland	Benzene	Traffic	EXPAND model combined with CAR-FMI Gaussian finite line source model	mean iF 10 ppm
Lobscheid et al., 2012	USA (65000 census tracks)	Primary conserved air pollutants	On-road mobile	S-R[a] relationships derived from AERMOD	mean iF 8.6 ppm
Tainio et al., 2014	Warsaw, Poland	7 pollutants, including PM	3066 sources; 14 categories: mobile, area, high point and other point	CALPUFF dispersion model	mean iF PM from mobile sources: 51 ppm; intraurban variability: 4–100 ppm
Lamancusa et al., 2017	USA	primary and secondary PM	25 source regions (including 10 cities)	CAMx regional air quality model	iD75 in most cities was < 50 km (except sulfates); primary $PM_{2.5}$ from urban areas: mean iD75 = 22 km, mean iF = 26 ppm)

[a] Source-receptor relationships.

exposures in 25 regions (10 cities with over 60 000 people, 6 smaller cities with population density over 286 km^{-2}, 3 rural regions with lower population density and 3 pristine regions in national parks). Over 75% of the intake for urban emissions occurred within 50 km (mean: 22 km) from the source for primary $PM_{2.5}$.

Two recent studies in Europe developed spatially-resolved iFs. In Helsinki, an approach combining dispersion modeling and spatial and temporal information on population activity patterns for a working-age population (494 000 people) using 100 × 100 m cells highlighted the dependence of iFs on population density (Loh et al., 2009). The overall iF was 10 ppm, between a 7 ppm box model estimate and a 39 ppm estimate derived using personal monitoring data (n = 129 persons). In Warsaw, iFs for 3066 emission sources in various source categories, e.g., mobile, area and point, were estimated using CALPUFF and local meteorological data (Tainio et al., 2014). Mean emission-weighted iFs ranged from 0.013 to 51 ppm across the source categories, and 44 ppm for primary $PM_{2.5}$ emissions from mobile sources (range from 4 to 100 ppm).

Both the iF studies and the broader literature show that iF estimates for traffic-related primary $PM_{2.5}$ emissions are substantially higher in urban areas, and that a significant share of exposure occurs in the near-road environment (Greco et al., 2007b; Zhang and Batterman, 2010; Lamancusa et al., 2017). Consequently, city-wide iF estimates (and dispersion-based models with coarse resolution) do not represent the spatial variation in exposure to traffic-related air pollutants, which is governed by population density, the distribution of emissions, and meteorological conditions (Marshall and Nazaroff, 2006; Greco et al., 2007a; Zhang and Batterman, 2010; Lobscheid et al., 2012). These factors may require site-specific analyses using dispersion or other types of spatially-resolved models to produce the concentration field, followed by the use of GIS to address spatial variations in population density and other factors that affect exposure (Reyna et al., 2015; Vienneau et al., 2009). While dispersion models can support health impact estimates, their application has been limited due to their complexity, time and resource requirements (Milando et al., 2016).

3. Materials and methods

3.1. Study site

The Lisbon metropolitan area (38° 24′ 32″ - 39° 03′ 52″ N, 08° 29′ 27″ - 09° 30′ 01″ W) is located on the western coast of Portugal. In 2011, it encompassed 18 municipalities, 211 parishes and 34 937 statistical subsections (referred to as “census blocks”), with a total population of 2 821 876 and an area of 3002 km^2 (940 km^{-2}); Lisbon city had 547 733 people and 85 km^2 (6448 km^{-2}) (INE, 2013). Winds occur mostly from the north and northwest, in particular during the *nortada*, which occurs on 45% of summer and spring days, with wind speeds above 5 m/s (Lopes et al., 2013). Meteorological data (NOAA, 2012, 2016) was obtained for the Lisboa/Gago Coutinho station (station reference POM0008579, coordinates 38.7667, −9.1333), which is at the Lisbon airport, near the city center. Census data used the geographic coordinate system GCS ETRS 1989 and the projected coordinate system ETRS 1989 TM06 Portugal (INE, 2013). These coordinate systems were maintained for all map data in the study (data using other systems was converted).

3.2. Spatially-resolved intake fraction estimates

Spatially-resolved iF estimates were derived for the metropolitan Lisbon area by combining several tools and datasets and modeling emissions, concentrations and the resulting exposures. In brief, traffic activity, fleet data and emission factor models were used to calculate road emissions; road configuration and local meteorological data were used in dispersion modeling to predict concentrations in specific buffers along roads; and demographic and activity data were used to estimate

population intake. The iF at hour t is:

$$iF_t = \sum_{i=1}^{n} \frac{P_{i,t} \times Q_{i,t} \times C_{i,t}}{E_{i,t}} \quad (1)$$

where $P_{i,t}$ = population, $Q_{i,t}$ = breathing rate per person (m^3/h), $C_{i,t}$ = mean hourly ambient concentration (μg/m^3), and $E_{i,t}$ = road emissions (μg/h) for hour t and location i. Location i refers to "cells" that result from the intersection of census tracks and road buffers (ranging up to 500 m from the road network, as described in the next section). Areas of these cells ranged from 0.22×10^{-3} m^2 to 2.6 km^2 (mean: 14 816 m^2), and they contained from 0 to 865 inhabitants (mean: 32). To account for the temporal variation in emissions (traffic activity), meteorological conditions and population activity patterns, four periods over the day were considered (Brito, 2012; INE, 2001): (1) night-time (8 p.m.–6 a.m., 10 h), (2) morning commute (6–10 a.m., 4 h), (3) day-time (10 a.m.–4 p.m., 6 h) and (4) evening commute (4–8 p.m., 4 h). The population, breathing rate, emissions and concentrations vary for these periods, as described below.

3.2.1. Road network and buffers

The road network modeled for the Lisbon metropolitan area included all roads for which there was publicly available traffic data (IMTT, 2016; TIS-CML, 2015; APA, 2015), which includes freeways and major arterials. The spatial configuration of the road network was based on OpenStreetMap© road data (OSM, 2017). A total of 601 km of road length, broken down into 181 road segments, were represented in the GIS (see supplementary materials). To calculate near-road exposures, four (mutually exclusive) buffers were defined on each side of the road's centerline at distances of 10 to 50, 50 to 100, 100 to 200 and 200 to 500 m. At road crossings, buffers were intersected to account for emissions from the two roads. For areas within 500 m of three or more major roads, only two roads were considered; this applied to few areas.

3.2.2. Road emissions

Road emissions were estimated by combining daily mean traffic volumes, disaggregated by road segment, with temporal traffic activity profiles and fleet emission factors. Table 3 summarizes the fleet composition, annual travel distance and emissions, by the main vehicle groups. Daily mean traffic volumes were obtained from public reports (IMTT, 2016; TIS-CML, 2015; APA, 2015). Simplified hourly temporal profiles for passenger and commercial traffic activity were developed (Fig. 1), based on the daily variation of traffic flows in Lisbon (Brito, 2012), resembling profiles developed elsewhere (Batterman, 2015; Batterman et al., 2015; Roh et al., 2016). Based on annual km-traveled, passenger vehicles accounted for 73% of the traffic, and commercial vehicles accounted for 27% (Ntziachristos et al., 2008). Temporal profiles considered only weekdays, as the day-time population distribution was based on commuting patterns (Section 3.2.4). Weekend patterns differ, e.g., the morning commuting period is absent, and most traffic occurs in the afternoon and evening periods (see supplementary materials).

Table 3
Summary of the national fleet composition and annual travel distance (2013) (Ntziachristos et al., 2008), and emission factors (modeled).

	Stock (10^3 vehicles)	Fleet annual travel distance (10^6 km)	Emission factors (mg/km)	
			National road	Highway
Passenger vehicles	5192	56 512	24	22
Passenger cars	4675	54 553	23	21
Mopeds and motorcycles	502	1542	29	28
Buses	15	417	145	110
Commercial vehicles	1354	20 818	50	64
Light commercial vehicles	1219	17 511	43	62
Heavy duty trucks	135	3307	90	75

Emission factors for the 2013 Portuguese fleet (Ntziachristos et al., 2008) were estimated using the EMEP/EEA Inventory guidebook (EEA, 2016), which provides models for exhaust emissions, gasoline evaporation and road tire and brake wear. The tier 3 model implemented in COPERT 5 software (Ntziachristos et al., 2009) was used to calculate exhaust and non-exhaust emissions based on technical and fleet activity data, e.g., vehicle technologies and mileage split. (Tiers 1 and 2 use simplified models that apply default values for many variables.) Meteorological and vehicle speed data are provided in the supplementary materials.

3.2.3. Near-road exposure concentrations

Ambient concentrations from traffic-related emissions were estimated in each buffer using an efficient dispersion modeling approach. First, we determined the mean orientation of each road segment using GIS, which was then classified into one of four directions (north – south, N-S; east – west, E-W; southwest - northeast, SW-NE; and southeast – northwest, SE – NW). Then, the Research LINE-source model (RLINE), a line source model specifically developed for traffic emissions and the near-road environment (Snyder et al., 2013), was used to calculate emission-to-concentration (or "transfer") coefficients for each road direction and distances up to 500 m from the road, using a line of receptors placed perpendicularly to the road segment at 5 m intervals (15–500 m from the road) on both sides (196 receptors). The road segment was modeled as a 3 km long linear source with unit emissions (1 g m^{-1} s^{-1}). The receptor height was 2.5 m. Concentrations were predicted using RLINE's numerical calculation option and hourly Lisbon surface and upper air meteorological data (NOAA, 2012, 2016) processed by the AERMET surface meteorological processor (Cimorelli et al., 2005). A total of 14 954 h of Lisbon meteorological data was modeled, representing about 85% of the hours in 2001–2002. (This period was selected based on completeness of the data available; by day period, data completeness ranged from 78 to 93%.) RLINE predictions were then averaged in each of four buffers (Section 3.2.1) and divided by the emission rate to provide the hourly transfer coefficients. The coefficients were averaged by each day period, segment direction and buffer distance, resulting in 128 transfer coefficients (4 road directions × 4 buffers × 2 sides of road × 4 day periods). Lastly, concentrations were determined as the product of the road segment emission rates and the transfer coefficients at the desired location, considering the distance and direction from the road.

This approach estimates annual average concentrations for areas within 500 m of major roads using only four archetype segments and geographic data. This approach is computationally efficient, an important consideration given the number of road segments, receptors and hours needed to develop long-term estimates in urban areas. Sensitivity analyses were performed to evaluate how the buffer size, the road orientation estimate, and the assumed segment length influenced results.

3.2.4. Background concentration

The RLINE dispersion modeling accounted for emissions on the larger roads and predicted concentrations to a distance of 500 m from the road. To account for emissions from smaller roads, and for roads beyond 500 m, a one-compartment model was used with the assumption that the "far-field" environment is well-mixed. This provided an hourly "background" concentration for the metropolitan area, calculated as:

$$C_t = \frac{E_t}{V_t} \quad (2)$$

where C_t = mean hourly concentration (μg/m^3) at hour t, E_t = total

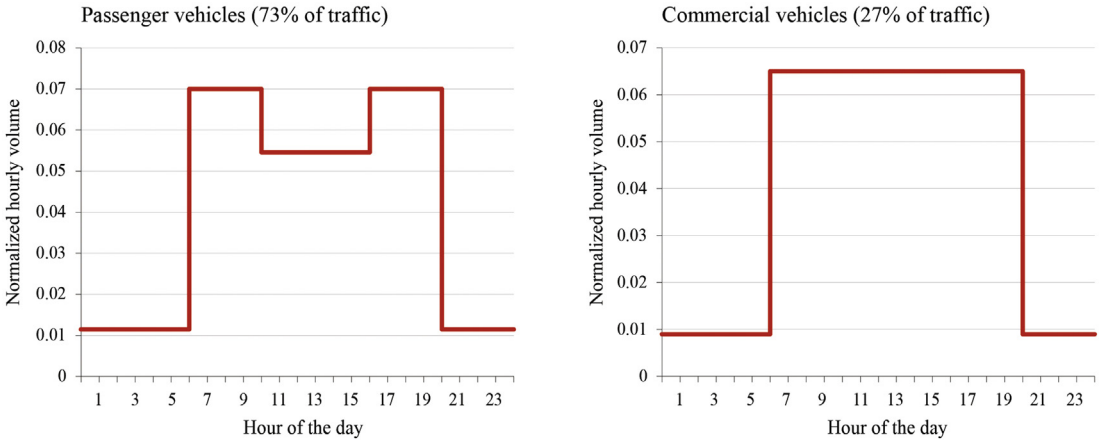

Fig. 1. Temporal profile of traffic volumes for passenger and commercial vehicles.

road emissions (μg/h) and V_t = ventilation rate (m^3/h) for hour t (Section 3.3). Hourly results were averaged for the four day periods into a 24-h mean. The background concentration, which is assumed to be uniform across the modeled domain, "double counted" contributions from the 3 km segment used to model the near-road concentration at each buffer, however, this contribution was negligible, less than 1% of the background estimate. (Mean emission rates of the 3 km segment ranged from 50 to 338 g/h for night and commuting periods, respectively, while the network total emission rates ranged from 7700 to 47 900 g/h.). Double counting could be eliminated using site-specific background estimates that removed the emissions from the 3 km segments modeled using RLINE.

3.2.5. Population distribution

Block-level demographic data was used to map the population distribution into "cells", defined as the intersection of census blocks and buffers (Section 3.2.3). The population in each cell was calculated for day- and night-time periods to account for workers (many of whom work in the urban core) and residents (who tend to be more dispersed in suburban areas). The population of most of the 18 Lisbon area municipalities decreases during the day (up to 28% depending on municipality), while the Lisbon city population increases (by 56%; INE, 2013). Census data were assumed to represent the night-time distribution of residents, and day-time population distribution was based on origin and destination of commuting trips at the municipality level (INE, 2013). Because information describing population shifts at high resolution was unavailable, a relatively simple mapping procedure was used to allocate the day-time population to census blocks. The day-time population was assumed to include the share of residents remaining in the block (those who did not work or study and those who worked or studied at home), and workers and students in the municipality. The population working or studying in each municipality was allocated to blocks based on the number of buildings of various types in the block weighted by a factor intended to reflect the number of workers: exclusively residential buildings, mainly residential buildings, and mainly non-residential buildings were assigned weights of 1, 3 and 6, respectively (INE, 2013). The population density was assumed to be uniform within each census block after excluding a 10 m buffer along the road axis.

3.2.6. Breathing rates

Age- and gender-specific breathing rates were estimated for day- and night-time periods using the Lisbon demographic data (Table 4; US EPA, 2011, 2009). Day-time rates, which averaged 0.80 m^3/h (moderate activity), were assumed for day-time, including both commuting periods (6 a.m.–8 p.m.); the night-time breathing rate was 0.34 m^3/h (passive activity).

Table 4
Population age and gender distribution in Lisbon metropolitan area and breathing rates, based on INE (2013), US EPA (2011) and US EPA (2009).

Group	Population	Breathing rates (m^3/d)		
		Night-time (10 h)	Day-time* (14 h)	24-h mean
Children				
0-14	437 881	6.38	15.26	11.56
Men				
15-24	148 856	9.56	23.04	17.42
25-64	748 913	9.64	22.91	17.38
> 65	213 260	9.02	19.12	14.91
Women				
15-24	146 187	7.96	19.13	14.48
25-64	826 197	7.55	18.64	14.02
> 65	300 582	6.75	14.71	11.39
Total	2 821 876	8.08	19.12	14.52

* includes commuting periods.

3.3. City-wide single iF estimate: one-compartment model

For comparison with the spatially-resolved estimate, a city-scale single iF was calculated using a one-compartment model:

$$iF = \frac{P \times Q_b}{V} \quad (3)$$

where P = population, Q_b = breathing rate per person (m^3/s), and V = ventilation rate (m^3/s). The population was based on census data (INE, 2013), and the breathing rate used the average in Table 4 (14.5 m^3/d; Section 3.2.5). The ventilation rate V (m^3/s) was calculated as:

$$V = \mu \times H \times W \quad (4)$$

where μ = mean wind speed (m/s), H = mixing height (m), and W = width in crosswind direction (m). Hourly mixing heights for the mechanically generated boundary layer were calculated using AERMOD (Cimorelli et al., 2004) from twice daily radiosonde observations for 2001 and 2002 (NOAA, 2016). Hourly surface observations of wind speed for the same period (NOAA, 2012) were extrapolated to the hourly mixing height using a power law coefficient of 0.32 and a cut-off height of 200 m, above which the wind speed was assumed constant (Apte et al., 2012). A total of 16 026 h had valid data (90% of the hours in the 2-year period, and 89–95% by day period). Surface wind speeds below 0.5 m/s and mixing heights below 50 m were excluded. The wind speed at 10 m height averaged 3.6 m/s (range: 0.5–13 m/s), and the mixing height averaged 1317 m (range: 61–4000 m). The dilution rate was calculated as the harmonic mean of

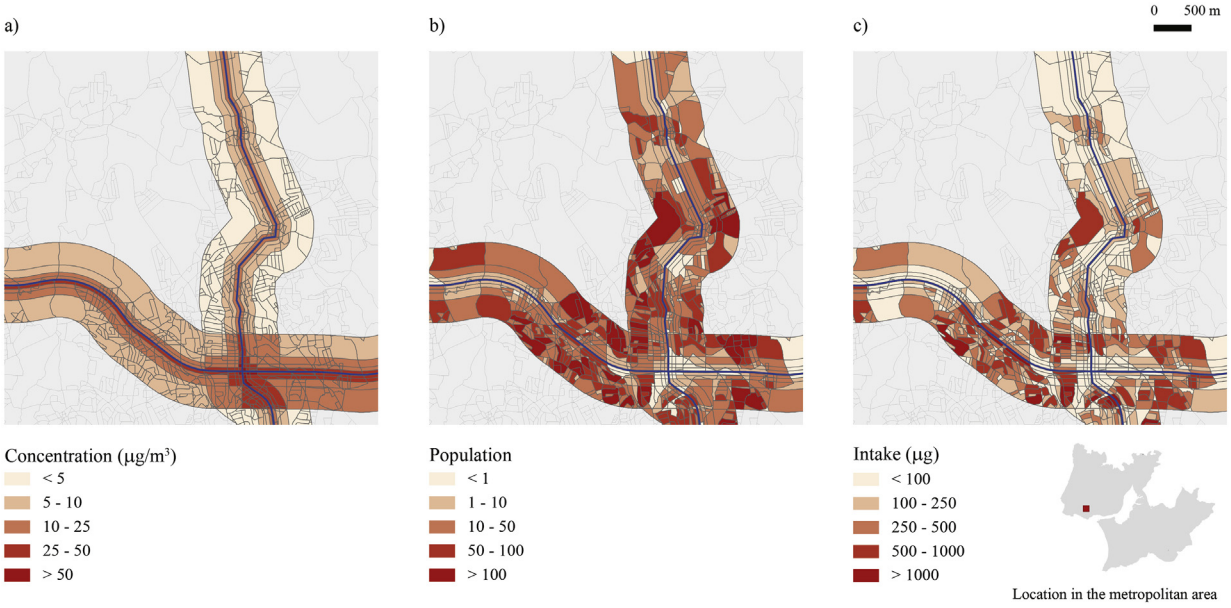

Fig. 2. Example of development of spatially-resolved iFs in Lisbon metropolitan area, showing 24-h mean (a) ambient concentrations, (b) near-road population and (c) intake. Includes near-road and background concentrations.

the hourly product of μ and H (Apte et al., 2012; Stevens et al., 2007). Width W was considered to be 55 km, the square root of the area, assuming a square domain. iF estimates were calculated with average daily parameters, and also using emissions and ventilation parameters specific to the four time periods used in the spatially-resolved approach.

4. Results and discussion

4.1. Spatially-resolved intake fraction estimates: dispersion-based model

Fig. 2 demonstrates the development of iF estimates for a small section of Lisbon containing several road segments. RLINE concentrations in the near-road buffers (panel *a*) are applied to the number of individuals in the cells (panel *b*, average of day and night-time populations by cell), giving $PM_{2.5}$ intake for the near-road population (panel *c*). This variation, which is fairly typical, shows the dependence on the population distribution, especially in the near-road environment. While concentrations along roads have fairly similar patterns with some nuances (e.g., concentrations may be higher on one side of a road due to prevailing winds), the population distribution can be highly heterogeneous. Since intake is the product of concentrations and population (neglecting the variation in breathing rates and other factors), intake tends to be very heterogeneous. Thus, cells with high population density can have high intake, even in buffers distant from the road or near low traffic roads. Such results show the importance of local data, in particular, the population size near busy roads.

Of the population living or working near roads (night- and day-time), about 5% were within 50 m, 8% within 50–100 m, 21% within 100–200 m and 65% within 200–500 m. These buffers corresponded to 9, 11, 21 and 58% of the total buffer area, respectively (491 km^2, equal to 16% of the Lisbon metropolitan area). (About 11% of cells were vacant, resulting in no intake, i.e., iF = 0). Diurnal population shifts decreased the iF by about 13% compared to the use of residence (Census) locations alone, reflecting that 1.047 million people live within 500 m of large roads, but only an estimated 0.893 million are within 500 m during the day.

Table 5 summarizes predicted concentrations and iF estimates for the population living or working within 500 m from roads. 24-hour $PM_{2.5}$ concentrations averaged 0.65 µg/m^3 across the 33 230 cells (range: 0.36 µg/m^3 at night and 1.76 µg/m^3 during the morning commuting period); cells near large roads with high traffic volumes had much higher concentrations. Concentrations at night and during daytime periods were much lower than those during commuting periods (Fig. 3), reflecting effects of emission and ventilation rates. Emission rates are low at night (7.7 kg/h for the modeled road network) and increase during commuting periods (47.9 kg/h), while mid-day emissions are just slightly lower (41.6 kg/h). However, dispersion increases considerably during the daytime periods, which tends to lower concentrations. This diurnal pattern has the effect of lowering iF estimates compared to those estimated using constant emissions. This variation depends on both the daily emission profile and prevailing meteorological conditions, e.g., other areas that have frequent and strong nocturnal inversions during the morning will show greater differences between morning and evening commuting periods, and areas with shorter and earlier evening commuting periods may have lower concentrations in the evening.

The overall iF for the metropolitan Lisbon is 16.4 ppm, which includes the near-road exposure iF contribution of 12.0 ppm (using a night- and day-time populations of 1.05 and 0.89 million, respectively), and the far-field exposure iF contribution of 4.3 ppm (population of 1.77 and 1.93 million beyond 500 m of the modeled road network in night- and day-time, respectively). Thus, most (74%) intake occurs within 500 m of major roads. This near-road region represents 16% of the study area and contains 31–38% of the population.

4.2. City-scale intake fraction estimate: one-compartment model

The iFs calculated using the one-compartment models are shown in Table 6. With the steady state model, iF estimates for Lisbon (9.3 ppm) and the larger metropolitan area (8.1 ppm) are very similar, although on a per person basis there is a 6-fold difference. Compared to Lisbon city, the ventilation rate is about 6 times higher across metropolitan Lisbon (corresponding to the width difference), but the population is 5 times greater. These factors offset each other in the iF calculation. These estimates do not incorporate the temporal variation in the emission profiles.

The one-compartment model with hourly variation in the dilution rates and emissions provided an iF estimate of 6.5 ppm, slightly lower than the steady-state one-compartment model iF of 8.1 ppm. (The former estimate uses the same breathing rates, emission and dilution

Table 5
Summary of spatially-resolved analysis showing cell size, population, predicted concentrations and iFs for cells within 500 m of major roads. Based on 33 230 cells. Concentrations and intake rates include RLINE and background estimates.

	Units	Mean	St.dev.	Min	P10	P25	P50	P75	P90	Max
Cell area	m^2	14 816	51 237	0	199	1288	4258	11 330	29 934	2 629 723
Night population density	km^{-2}	7681	11 704	0	0	91	2032	10 276	25 156	113 804
Day population density	km^{-2}	6586	10 109	0	0	162	2396	9322	18 906	168 464
Night population		32	64	0	0	0	6	32	94	865
Day population		27	51	0	0	0	7	32	75	901
Mean hourly concentration	$\mu g/m^3$									
Night		0.363	0.332	0.066	0.104	0.146	0.254	0.455	0.767	3.680
Morning commuting		1.756	1.696	0.331	0.493	0.658	1.193	2.160	3.740	19.068
Day		0.589	0.963	0.045	0.063	0.091	0.202	0.668	1.534	12.121
Evening commuting		0.972	1.250	0.100	0.165	0.245	0.514	1.204	2.344	15.090
24-h mean intake	µg/d	257	636	0	0	4	50	228	655	15 715
iF	ppt	362	895	0	0	6	71	321	922	22 121
$iF_{personal}$	ppt	18	22	1	4	5	10	21	41	325

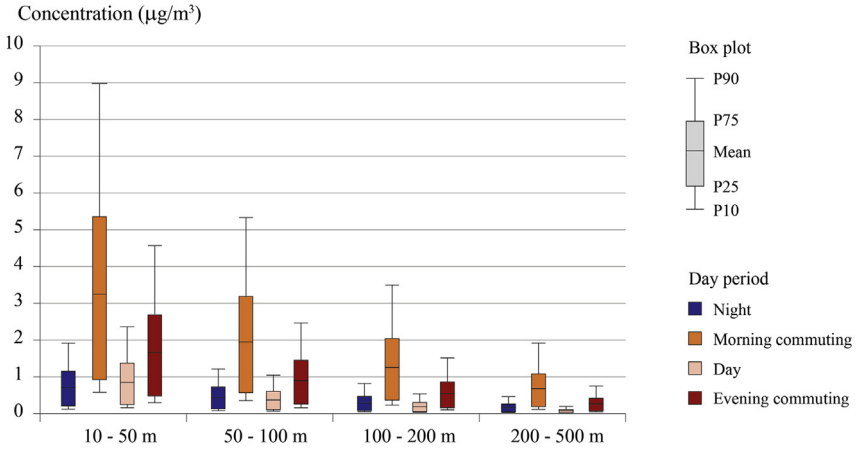

Fig. 3. Mean $PM_{2.5}$ concentrations due to near-road emissions for four buffers and four day periods. Plots show mean, 10th, 25th 75th and 90th percentile concentrations.

rates as the spatially-resolved iF estimates.) At night, breathing rates and emissions are low, which tend to offset the lower night-time dilution rates. During the day, emissions increase considerably (together with breathing rates), however, dilution rates also increase due to faster winds and higher mixing height.

4.3. Comparison of iF estimates

The one-compartment iF estimates for metropolitan Lisbon (steady-state model: 8.1 ppm, temporally-disaggregated model: 6.5 ppm) are less than half that estimated using the spatially-resolved approach (16.4 ppm), and only slightly more than the 4.3 ppm estimate for the far-field population (1.8 million people, 64% of the overall population). Near-road exposure accounted for 74% of the spatially-resolved iF (population of 0.96 million living within 500 m from major roads, 34% of the overall population and 16% of the domain area) and far-field exposure accounted for 26% (population of 1.86 million living beyond 500 m of the modeled road network).

The iF values for Lisbon are at the low end of the literature range for urban areas (Section 2), a result of Lisbon's relatively low population density and high dilution rate. In earlier work examining many cities, Apte et al. (2012) estimated an iF of 13.5 ppm for Lisbon (the study published mean results for cities aggregated by world region; data for Lisbon was obtained by private communication), which applied to a population of 1.9 million people in a 222 km^2, giving a population density of 8748 km^{-2}. In contrast, we considered the entire

Table 6
Parameters and results for the one compartment iF steady-state and emission-weighted model (with hourly variation of dilution rates and emissions).

Domain	Area	Width	Population	Population density	Breathing rate	Dilution rate	iF	iF personal
	(km^2)	(km)	(million)	(km^{-2})	(m^3/d)	(m^2/s)	(ppm)	(ppt)
Steady-state model								
Lisbon metropolitan area	3002	55	2.82	940	16.0	1069	8.1	2.9
Lisbon city	85	9	0.55	6444	16.0	1069	9.3	17.1
*Emission-weighted model**								
Night-time	3002	55	2.82	940	8.1	672	7.2	2.5
Morning commuting	3002	55	2.82	940	19.1	808	14.1	5.0
Day-time	3002	55	2.82	940	19.1	4969	2.3	0.8
Evening commuting	3002	55	2.82	940	19.1	2763	4.1	1.5
24-h mean	3002	55	2.82	940	14.5	2118	6.5	2.3

* Lisbon metropolitan area.

metropolitan area with a population of 2.8 million and an area of 3002 km^2, giving a population density of only 940 km^{-2} (Table 6). On a per person basis, our $iF_{personal}$ estimate is 2.9 ppt, less than half of the earlier estimate (7.0 ppt).

As noted earlier, iFs based on one-compartment models are sensitive to the domain selected, which ideally should correspond to the scope and goal of the study. In this study, iF estimates considered exposure to traffic-related air pollutants across the Lisbon metropolitan area, and administrative borders were used to define the domain. In contrast, Apte et al. (2012) based the land area and city population on a dataset derived from satellite mapping of built land cover, and obtained a population density that exceeded those in any of the 18 municipalities that comprise metropolitan Lisbon (139 km^{-2} in *Alcochete* to 7389 km^{-2} in *Amadora*; INE, 2013). Satellite-based estimates can differ significantly from administrative boundaries, e.g., parks, forested and water areas may be excluded within an urban area (Angel et al., 2010; Schneider et al., 2009). Excluding such areas, which increases the population density with the effect of increasing the iF, may be appropriate for traffic-related emissions since exposure and intake occurs near the source. However, results can depend on the scale and urban form. The similarity between our dispersion modeling-based iF and Apte et al.'s (2012) results might be fortuitous. Two urban settlements with the same area and population but different urban forms (e.g., road configuration and population distribution) could have significantly different iFs when spatially-resolved, but very similar iFs using a one-compartment model.

The high dilution rate in Lisbon is reflected in the one-compartment model iF estimate. Mixing heights in Lisbon generally exceed values used in one-compartment modeling (Table 1). Our 2001–2002 data shows mean and median mixing heights of 1317 and 1144 m, respectively, which are consistent with previous Lisbon 1999–2000 monthly-averaged midday mixing height estimates (843–1465 m) using radiosonde data (Baklanov et al., 2005), and also with the mean height (1219 m) of the first inversion layer derived from twice daily radiosonde observations for Lisbon in 2001–2002 (NOAA, 2016). Our dilution rate (harmonic mean of 1069 m^2/s) also is comparable to the 1130 m^2/s calculated by Apte et al. (2012) for Lisbon using the NASA MERRA database (Rienecker et al., 2011).

4.4. Sensitivity analyses

Several sensitivity analyses were completed for key modeling parameters. First, analyses using four road orientations (range ± 22.50°), presented previously, were compared with the use of eight orientations (range ± 11.25°). The latter increased 24-h mean concentrations by an average of 3–6% across the four day periods, and increased the overall near-road iF by 11% (12.0–13.4 ppm). This suggests that RLINE modeling might benefit from additional road orientations. The effect of the number of orientations will depend on the road configuration and meteorological variables (especially wind direction), but handling additional orientations in the modeling framework is not difficult.

Second, to examine the effect of buffer size or resolution, we modeled an east-west road in western Lisbon (highway A5; 25.6 km, 11 segments) and compared iF estimates for the four buffers used previously (cut-offs at 50, 100, 200 and 500 m) with results from two other sets of buffers: two large buffers (cut-offs at 200 and 500 m), and eight small buffers (25, 50, 75, 100, 150, 200, 350 and 500 m). The three sets of buffers used 1 808, 1340 and 2875 cells, respectively. Compared to the 4-buffer case, the 2-buffer model increased iFs by 17%, while the 8-buffer case decreased iFs by 25%. While results might differ from other roads and areas for Lisbon, these results demonstrate the sensitivity to buffer size or resolution, and indicate the need for highly-resolved analyses near major roads. While a larger number of buffers is potentially more accurate, we generally do not know where individuals reside or work with precision. Further investigation on buffer size is warranted.

A third sensitivity analysis examined how the segment road length used by RLINE affected results. Compared to the 3 km segment used, a 1 km segment decreased mean concentrations by 16–17% (averaged across 33 230 cells and four day periods), and the overall near-road iF (including background concentration) decreased by 20%. With a 10 km segment, mean concentrations increased by 6–7% and the iF increased by 8%. The 3 km segment length, which represents a compromise with respect to modeling the actual road geometry, captures the bulk of the near-road impacts.

Fourth, to compare results obtained using dispersion modeling to the one-compartment model used for background and far-field concentrations, we added an additional buffer for distances from 500 to 1000 m from the road using receptors on 50 m centers. The added buffer contained 14 744 cells and 693 000 to 770 000 people (for day- and night-time periods, respectively), representing 25–27% of the metropolitan Lisbon population. In this buffer, the mean concentration was 0.14 $\mu g/m^3$ and the iF was 2.7 ppm, equal to a 40% increase in concentration and a 58% increase in the iF for this population compared to the one-compartment model (which yielded a concentration of 0.10 $\mu g/m^3$ and an iF of 1.7 ppm). Thus, extending the dispersion modeling domain increased the iF of the overall urban population compared to simple one-compartment models, although the bulk of exposure (69%) occurs within 500 m of roads. Differences are expected to decrease, however, as the buffer size increases since predicted concentrations decrease with distance.

These analyses suggest that overall errors caused by discretizing road segments by direction and using a standard length can be on the order of 10% on average and that utilizing a number a limited number of buffers may cause larger errors, perhaps on the order of 25% on average and potentially higher for some subgroups or in some buffers. Due to data gaps and the computational challenge, we did not model the actual road network or use a highly resolved receptor grid to calculate iFs, which might serve as a reference case. The sensitivity analyses help to identify possible error sources and support our major conclusion, that is, the importance of near-road exposures.

4.5. Computational considerations

The RLINE dispersion modeling for Lisbon required four 2-year runs for each road direction and the 196 receptors; these runs were completed within 10 h on a PC workstation. In contrast, modeling the metropolitan area with the 601 km road network would require about 1.2 million receptors using a 50 m grid or 195 000 receptors for the near-road (within 500 m) area, presenting an enormous computation burden.

4.6. Main strengths and limitations

This paper presents an innovative and efficient approach for estimating iFs that account for near-road exposure to traffic-related air pollutants using local and spatially-resolved emission and demographic data. The approach represents the small-scale spatial variation in concentrations and population density, which is important for intake and impact estimates for traffic-related air pollutants since most exposure occurs near major roads. In addition, the approach does not have the scale or domain sensitivity observed in simple one-compartment models. Thus, the suggested approach appears to be more accurate and robust than one-compartment models and coarse resolution dispersion models, which have strong scale dependencies and which do not account for spatial heterogeneity.

In addition to estimating the overall intake and iF, the spatially-resolved approach identifies the areas where intake and exposure rates are high. This information can inform and support decision-making in transportation and urban planning. For example, it can be used to map and prioritize areas and roads for traffic management policies (e.g., tolls, reduced speeds, time or fleet restrictions on specific roads or

zones); inform road infrastructure and transit planning to account for health impacts, and in a development context, target areas with lower exposures for urbanization and densification. More generally, spatially-resolved analyses are required to assess exposure and health disparities, and to evaluate and resolve potential environmental injustice issues in which vulnerable populations (e.g., by race/ethnicity, or socio-economic level) are associated with higher exposures and adverse health consequences (Hajat et al., 2015; Pratt et al., 2015; Kravitz-Wirtz et al., 2016).

A third important strength is the computation efficiency of the approach. The use of RLINE, considered to be a state-of-the-science dispersion model for near-road applications (Snyder et al., 2013), involves considerable computation and large-scale applications using this model are difficult. We modeled a large area by pre-computing transfer coefficients for different road alignments. Factors that might be considered to increase the accuracy include additional road-angles, segment lengths, smaller buffers, and terrain and road features (e.g., road grade).

Our analysis required a number of simplifications and assumptions, mainly due to the lack of publicly available data. The road network was incomplete, traffic-activity profiles were simplified, the day-time population was approximated, national fleet data and emission factors were used, and congestion was not considered. Only major streets were modeled. While these account for the bulk of emissions, the use of a more detailed and complete road network could improve accuracy. Accuracy could be improved using link-specific emissions inventory data, Lisbon-specific fleet information, more detailed population activity patterns, and the inclusion of on-road exposure. An improved emissions inventory might include spatially-resolved traffic-activity data (e.g., vehicle type, age, speeds, etc.). Despite the simplifications and assumptions made in the present analysis, our iF estimates appear more accurate than those based on simple box models.

We also simplified the dispersion modeling, in part to address data gaps and to increase computational efficiency. The RLINE model, like other line source models, incompletely addresses influences of the urban form, such as effects from narrow roads, street canyons, channeling of winds, and other factors that can influence dispersion (Tang and Wang, 2007). The accuracy of dispersion models is highly dependent on the quality and relevance of meteorological data (Stevens et al., 2007), and the single meteorological site used might not be representative of the entire metropolitan area. In addition, mixing height and wind profile data were based on only two radiosonde measurements per day. We examined only traffic-related emissions and primary $PM_{2.5}$; modeling secondary PM could add significant complexity (Lamancusa et al., 2017), although iF estimates may not increase considerably (Greco et al., 2007b). Lastly, our background estimates (attributable to far-field traffic emissions) used a simple box model, which does not account for possible gradients in the far-field, and it double counted emissions from the near-road road segment, however, this was shown to have negligible (< 1%) impact. Using four archetype road segments and discretizing dispersion modeling outputs into only four buffers significantly increased efficiency; however, the use additional alignments and smaller (narrower) buffers could improve accuracy.

Additional limitations reflect the use of ambient concentrations as a measure of personal exposure. We did not account for time-activity data and outdoor-indoor penetration of pollutants (Dons et al., 2011; Tainio et al., 2014; Requia, Adams et al., 2017). On-road exposures and traffic congestion were not considered. Urban scale iF estimates have yet to account for these types of effects.

5. Conclusions

We present a novel approach for estimating spatially-resolved iFs for traffic-related air pollutants that features a computationally-efficient dispersion model approach to account for near-road exposure and the population distribution. The overall iF estimate for the Lisbon metropolitan area, 16.4 ppm for $PM_{2.5}$, is nearly twice that based on one-compartment models for the same area. Most (74%) intake occurs within 500 m of major roads (16% of the domain) by a subset of the population (32–37%) living or working near large roads. Unlike the simplified one-compartment models, the suggested approach accounts for the temporal and spatial variability of emissions, accounts for population shifts over the day, identifies areas and populations that are highly exposed, and it appears robust with respect to the spatial domain considered.

This suggested approach can increase the accuracy of exposure and health effects estimates associated with traffic-related air pollutants. It demonstrates the importance of using local and spatially-resolved data for exposure and health impact estimates. The results can inform and support policies and decision-making addressing urban air quality and public health, particularly, transportation-related planning that can prioritize areas to decrease or displace emissions, such as road use fees, time or fleet restrictions on specific roads or zones and truck routing. It can also inform urban planning decisions by developing urbanization and densification strategies that minimize exposure.

Acknowledgements

This work is framed under the Initiative Energy for Sustainability of the University of Coimbra and the MIT Portugal Program. Joana Bastos is grateful for the financial support provided by the Foundation for Science and Technology (FCT), Portugal, through the doctoral degree grant SFRH/BD/52309/2013. The authors acknowledge support from FCT through the project SABIOS PTDC/AAG-MAA/6234/2014. Support for this research was provided by a grant from the Health Effects Institute, an organization jointly funded by the United States Environmental Protection Agency (EPA) (Assistance Award No. R-82811201) and certain motor vehicle and engine manufacturers. The contents of this article do not necessarily reflect the views of HEI, or its sponsors, nor do they necessarily reflect the views and policies of the EPA or motor vehicle and engine manufacturers. We acknowledge additional support from grant P30ES017885 from the National Institute of Environmental Health Sciences, National Institutes of Health, and grant T42 OH008455-10 from the National Institute of Occupational Health and Safety. Additional support for this research was provided under Research Agreement #4940-RFA13-1/14-1 by the Health Effects Institute, an organization jointly funded by the United States Environmental Protection Agency (EPA) (Assistance Award No. R-82811201) and certain motor vehicle and engine manufacturers.

Appendix A. Supplementary data

Supplementary data related to this article can be found at https://doi.org/10.1016/j.atmosenv.2018.07.037.

References

Angel, S., Parent, J., Civco, D.L., Blei, A.M., Potere, D., 2010. A Planet of Cities: Urban Land Cover Estimates and Projections for All Countries, 2000-2050 (No. WP10SA3). A Planet of Cities.

APA, 2015. Tabela das grandes infrastruras de transporte rodoviário. [Table of the large infrastructures of road transport, in Portuguese]. Agência Portuguesa do Ambiente.

Apte, J.S., Bombrun, E., Marshall, J.D., Nazaroff, W.W., 2012. Global intraurban intake fractions for primary air pollutants from vehicles and other distributed sources. Environ. Sci. Technol. 3415–3423. https://doi.org/10.1021/es204021h.

Baklanov, A., et al., 2005. The Urban Surface Energy Budget and Mixing Height in European Cities: Data, Models and Challenges for Urban Meteorology and Air Quality. Final Report of Working Group 2 of COST-715 Action. Demetra Ltd Publishers.

Batterman, S., 2015. Temporal and spatial variation in allocating annual traffic activity across an urban region and implications for air quality assessments. Transport. Res. Part D 41, 401–415. https://doi.org/10.1016/j.trd.2015.10.009.

Batterman, S., Cook, R., Justin, T., 2015. Temporal variation of traffic on highways and the development of accurate temporal allocation factors for air pollution analyses. Atmos. Environ. 107, 351–363. https://doi.org/10.1016/j.atmosenv.2015.02.047.

Bennett, D.H., McKone, T.E., Evans, J.S., Ni, M.L.E.D.M., Smith, K.R., 2002. Defining

intake fraction. Environ. Sci. Technol. https://doi.org/10.1021/es0222770.
Brito, J., 2012. Caracterização da flutuação do tráfego na cidade de Lisboa. Universidade Nova de Lisboa.
Cimorelli, Alan J., et al., 2004. AERMOD: description of model formulation. Report 44, 1–91 doi:EPA-454/R-03-004.
Cimorelli, A.J., et al., 2005. AERMOD: a dispersion model for industrial source applications. Part I: general model formulation and boundary layer characterization. J. Appl. Meteorol. 44, 682–693. https://doi.org/10.1175/JAM2227.1.
Dons, E., Int Panis, L., Van Poppel, M., Theunis, J., Willems, H., Torfs, R., Wets, G., 2011. Impact of time-activity patterns on personal exposure to black carbon. Atmos. Environ. 45, 3594–3602. https://doi.org/10.1016/j.atmosenv.2011.03.064.
EEA, 2017. Air Quality in Europe – 2017 Report. EEA Report No. 13/2017. European Environment Agency (EEA). Publications of the European Union, Luxembourg. https://doi.org/10.2800/850018. ISSN 1977-8449.
EEA, 2016. EMEP/EEA Air Pollutant Emission Inventory Guidebook 2016: Technical Guidance to Prepare National Emission Inventories. European Environment Agency (EEA) Technical reporthttps://doi.org/10.2800/247535.
Greco, S.L., Wilson, A.M., Hanna, S.R., Levy, J.I., 2007a. Factors influencing mobile source particulate matter emissions-to-exposure relationships in the Boston urban area. Environ. Sci. Technol. 41, 7675–7682. https://doi.org/10.1021/es062213f.
Greco, S.L., Wilson, A.M., Spengler, J.D., Levy, J.I., 2007b. Spatial patterns of mobile source particulate matter emissions-to-exposure relationships across the United States. Atmos. Environ. 41, 1011–1025. https://doi.org/10.1016/j.atmosenv.2006.09.025.
Hajat, A., Hsia, C., O'neill, M.S., 2015. Socioeconomic disparities and air pollution exposure: a global review. Curr. Environ. Heal. Rep. 2, 440–450. https://doi.org/10.1007/s40572-015-0069-5.
Heath, G., Granvolg, P., Hoats, A., Nazaroff, W., 2006. Intake fraction assessment of the air pollutant exposure implications of a shift toward distributed electricity generation. Atmos. Environ. 40, 7164–7177. https://doi.org/10.1016/j.atmosenv.2006.06.023.
Humbert, S., et al., 2011. Intake fractions for particulate matter: recommendations for life cycle assessment. Environ. Sci. Technol. 45, 4808–4816. https://doi.org/10.1021/es103563z.
IMTT, 2016. Relatório de tráfego na rede nacional de autoestradas. 4o trimestre de 2015. Lisbon, Portugal.
INE, 2013. Censos 2011 - Resultados Definitivos. [Census 2011 – Definite Results, in Portuguese]. Instituto Nacional de Estatistica, Lisbon, Portugal [Statistics Portugal, in Portuguese].
INE, 2001. Inquérito à ocupação do tempo 1999. Principais resultados. Lisbon, Portugal.
Karagulian, F., et al., 2015. Contributions to cities' ambient particulate matter (PM): a systematic review of local source contributions at global level. Atmos. Environ. 120, 475–483. https://doi.org/10.1016/j.atmosenv.2015.08.087.
Kravitz-Wirtz, N., Crowder, K., Hajat, A., Sass, V., 2016. The long-term dynamics of racial/ethnic inequality in neighborhood air pollution exposure, 1990-2009. Du Bois Rev. Soc. Sci. Res. Race 13, 237–259. https://doi.org/10.1017/S1742058X16000205.
Lai, a C., Thatcher, T.L., Nazaroff, W.W., 2000. Inhalation transfer factors for air pollution health risk assessment. J. Air Waste Manag. Assoc. 50, 1688–1699. https://doi.org/10.1080/10473289.2000.10464196.
Lamancusa, C., Parvez, F., Wagstrom, K., 2017. Spatially resolved intake fraction estimates for primary and secondary particulate matter in the United States. Atmos. Environ. 150, 229–237. https://doi.org/10.1016/j.atmosenv.2016.11.010.
Lim, S.S., et al., 2012. A comparative risk assessment of burden of disease and injury attributable to 67 risk factors and risk factor clusters in 21 regions, 1990-2010: a systematic analysis for the Global Burden of Disease Study 2010. Lancet 380, 2224–2260. https://doi.org/10.1016/S0140-6736(12)61766-8.
Lobscheid, A., Nazaroff, W., Spears, M., Horvarth, A., McKone, T., 2012. Intake fractions of primary conserved air pollutants emitted from on-road vehicles in the United States. Atmos. Environ. 63, 298–305. https://doi.org/10.1016/j.atmosenv.2012.09.027.
Loh, M.M., et al., 2009. Intake fraction distributions for benzene from vehicles in the Helsinki metropolitan area. Atmos. Environ. 43, 301–310. https://doi.org/10.1016/j.atmosenv.2008.09.082.
Lopes, A., Alves, E., Alcoforado, M.J., Machete, R., 2013. Lisbon urban heat island updated: new highlights about the relationships between thermal patterns and wind regimes. Adv. Meteorol. 2013. https://doi.org/10.1155/2013/487695.
Marshall, J., Nazaroff, W., 2006. Intake fraction. In: Wallace, Lance A., Steinemann, A.C., Ott, W.R. (Eds.), Exposure Analysis. CRC Press, pp. 237–251. https://doi.org/10.1201/9781420012637.ch10.
Marshall, J., Riley, W.J., McKone, T.E., Nazaroff, W.W., 2003. Intake fraction of primary pollutants: motor vehicle emissions in the south coast air basin. Atmos. Environ. 37, 3455–3468. https://doi.org/10.1016/S1352-2310(03)00269-3.
Marshall, J.D., Teoh, S., Nazaroff, W.W., 2005. Intake Fraction of Nonreactive Vehicle Emissions in US Urban Areas, vol. 39. pp. 1363–1371. https://doi.org/10.1016/j.atmosenv.2004.11.008.
Milando, C.W., Martenies, S.E., Batterman, S.A., 2016. Assessing concentrations and health impacts of air quality management strategies : framework for Rapid Emissions Scenario and Health impact ESTimation (FRESH-EST). Environ. Int. 94, 473–481. https://doi.org/10.1016/j.envint.2016.06.005.
NOAA, 2016. Integrated Global Radiosonde Archive (IGRA). Version 2 [WWW Document]. https://www1.ncdc.noaa.gov/pub/data/igra/, Accessed date: 4 May 2017.
NOAA, 2012. Integrated Surface Database - Surface Data Hourly Global (DS3505). [WWW Document]. https://www.ncdc.noaa.gov/isd, Accessed date: 4 May 2017.
Ntziachristos, L., Gkatzoflias, D., Kouridis, C., Samaras, Z., 2009. COPERT: a European road transport emission inventory model. In: Athanasiadis, I.N., Rizzoli, A.E., Mitkas, P.A., Gomez, J.M. (Eds.), Environmental Science and Engineering. Springer Berlin Heidelberg, Berlin, Heidelberg, pp. 491–504. https://doi.org/10.1007/978-3-540-88351-7_37.
Ntziachristos, L., et al., 2008. European Database of Vehicle Stock for the Calculation and Forecast of Pollutant and Greenhouse Gases Emissions with TREMOVE and COPERT. Final Report. Thessaloniki, Greece.
OSM, 2017. OpenSreetMap© (OSM) Data Last Updated in 2017-04-17. Retrieved from: https://planet.openstreetmap.org.
Pratt, G.C., Vadali, M.L., Kvale, D.L., Ellickson, K.M., 2015. Traffic, air pollution, minority and socio-economic status: addressing inequities in exposure and risk. Int. J. Environ. Res. Publ. Health 12, 5355–5372. https://doi.org/10.3390/ijerph120505355.
Requia, W., Adams, M., Arain, A., et al., 2017a. Spatio-temporal analysis of particulate matter intake fractions for vehicular emissions: hourly variation by micro-environments in the Greater Toronto and Hamilton Area, Canada. Sci. Total Environ. 599–600 (2017), 1813–1822. https://doi.org/10.1016/j.scitotenv.2017.05.134.
Requia, W., Dalumpines, R., Adams, M., et al., 2017b. Modeling spatial patterns of link-based $PM_{2.5}$ emissions and subsequente human exposure in a large canadian metropolitan area. Atmos. Environ. 158 (2017), 172–180. https://doi.org/10.1016/j.atmosenv.2017.03.038.
Reyna, J.L., Chester, M., Ahn, S., Fraser, A., 2015. Improving the accuracy of vehicle emissions profiles for urban transportation greenhouse gas and air pollution inventories. Environ. Sci. Technol. 49, 369–376. https://doi.org/10.1021/es5023575.
Rienecker, M.M., et al., 2011. MERRA: NASA's modern-era retrospective analysis for research and applications. J. Clim. 24, 3624–3648. https://doi.org/10.1175/JCLI-D-11-00015.1.
Roh, H.-J., Sahu, P.K., Sharma, S., Datla, S., Mehran, B., 2016. Statistical investigations of snowfall and temperature interaction with passenger car and truck traffic on primary highways in Canada. J. Cold Reg. Eng. 30, 4015006. https://doi.org/10.1061/(ASCE)CR.1943-5495.0000099.
Schneider, A., Friedl, M.A., Potere, D., 2009. A new map of global urban extent from MODIS satellite data. Environ. Res. Lett. 4, 44003. https://doi.org/10.1088/1748-9326/4/4/044003.
Shneider, J., Nagi, C., Read, B., 2014. EU air quality policy and WHO guideline values for health. Dir. Gen. Intern. Policies. Policy Dep. A Econ. Sci. Policy. https://doi.org/10.1017/CBO9781107415324.004. Sutyd IP/A/ENVI/2014-06.
Snyder, M.G., Venkatram, A., Heist, D.K., Perry, S.G., Petersen, W.B., Isakov, V., 2013. RLINE: a line source dispersion model for near-surface releases. Atmos. Environ. 77, 748–756. https://doi.org/10.1016/j.atmosenv.2013.05.074.
Stevens, G., de Foy, B., West, J.J., Levy, J.I., 2007. Developing intake fraction estimates with limited data: comparison of methods in Mexico City. Atmos. Environ. 41, 3672–3683. https://doi.org/10.1016/j.atmosenv.2006.12.051.
Tainio, M., Holnicki, P., Loh, M., Nahorski, Z., 2014. Intake fraction variability between air pollution emission sources inside an urban area. Risk Anal. 34, 2021–2034. https://doi.org/10.1111/risa.12221.
Tang, U.W., Wang, Z.S., 2007. Influences of urban forms on traffic-induced noise and air pollution: results from a modelling system. Environ. Model. Software 22, 1750–1764. https://doi.org/10.1016/j.envsoft.2007.02.003.
TIS-CML, 2015. Requalificação da 2a Circular. Estudo de Tráfego – Modelo Macro.
US EPA, 2011. Exposure Factors Handbook: 2011 Edition. U.S. Environ. Prot. Agency EPA/600/R-, 1–1466. doi:EPA/600/R-090/052F.
US EPA, 2009. Metabolically Derived Human Ventilation Rates: a Revised Approach Based upon Oxygen Consumption Rates. U.S. Environmental Protection Agency, Washington EPA/600/R-06/129F.
Vienneau, D., de Hoogh, K., Briggs, D., 2009. A GIS-based method for modelling air pollution exposures across Europe. Sci. Total Environ. 408, 255–266. https://doi.org/10.1016/j.scitotenv.2009.09.048.
Watkiss, P., Pye, S., Holland, M., 2005. CAFE CBA: Baseline Analysis 2000 to 2020. CAFE Programe.
World Health Organization, 2016. Ambient Air Pollution: a Global Assessment of Exposure and burden of Disease. World Health Organization, pp. 131 ISBN 978 92 4 151135 3.
World Health Organization, 2013. Health effects of particulate matter: policy implications for countries in eastern Europe, caucasus and central asia. J. Korean Med. Assoc. 50, 20. https://doi.org/10.5124/jkma.2007.50.2.175.
World Health Organization, 2003. Health Aspects of Air Pollution with Particulate Matter , Ozone and Nitrogen Dioxide. Rep. a WHO Work. Gr. Bonn, Ger. 13–15 January 2003. EUR/03/5042688. https://doi.org/10.2105/AJPH.48.7.913.
Zhang, K., Batterman, S., 2010. Near-road air pollutant concentrations of CO and PM2.5: a comparison of MOBILE6.2/CALINE4 and generalized additive models. Atmos. Environ. 44 (14), 1740–1748. https://doi.org/10.1016/j.atmosenv.2010.02.008.